

INVESTIGATION OF NEAR-FAULT VS. FAR FIELD GROUND MOTION EFFECTS ON A SUBSTANDARD BRIDGE BENT

Austin Brown
M. Saïid Saïidi¹

University of Nevada, Reno

ABSTRACT

Previous research has shown that near-fault ground motions can cause extensive damage to reinforced concrete bridge structures. However, there has been little done in addressing the comparative effects of near-fault vs. far-field ground motions on reinforced concrete bridge structures. Two identical substandard bridge bents were tested under dynamic ground motions on the shake tables at the University of Nevada, Reno. One of the bents was tested under near-fault ground motion and the other under far-field motion. This paper presents the comparative results from the two tests.

KEY WORDS: substandard design, near-fault, far-field, comparative

1 INTRODUCTION

Recent earthquakes have demonstrated that near-fault ground motions can cause severe damage to bridge structures. The effects of near-fault versus far-field ground motions are not well understood. According to Somerville, near-fault ground motions differ from ordinary ground motions in that they often contain a long period velocity pulse and permanent ground displacement. These characteristics occur in the horizontal component perpendicular to the strike of the fault (Somerville 2002). The spike in velocity should generally exceed 60 in/sec (152cm/sec) in order for the motion to be classified as a near-fault ground motion. However, this is only an estimate and ground motions with lower peak velocities can be classified as near-fault ground motions as well. Another factor for classifying ground motions as ‘near-fault’ is the distance to the epicenter of the earthquake. The epicenter should be within 10 miles (approximately 15km) of a structure of interest.

The purpose of this study was to compare the effects of near-fault versus far-field ground motions on a substandard bridge bent. Two identical substandard bridge bent specimens were tested at the University of Nevada, Reno. The specimens represent a quarter-scale model of a bridge bent located in Las Vegas, Nevada. The first bent was designated B2DA for bent with two columns with diamond shape and as-built details. Testing of B2DA was reported in (Sureshkumar et al. 2004). The second bent was designated B2DN for bent with two columns with diamond shape and was tested under

¹ Professor, Dept. of Civil and Environmental Engineering, University of Nevada, Reno

near-fault ground motion as part of a current study. Both specimens were tested in the strong direction of the bent until failure. B2DA was subjected to the far-field acceleration history recorded at the Sylmar receiving station during the 1994 Northridge earthquake. B2DN was subjected to the near-fault acceleration history recorded at the Rinaldi receiving station during the 1994 Northridge earthquake. Several parameters were used to study the effects of near-fault versus far-field ground motions. A visual inspection and comparisons were completed. Throughout testing, photos were taken in order to document the visual damage to the specimens. The photos were compared and damage was assessed based on cracking of concrete and visual failure mechanisms. In addition, the force-displacement responses for the specimens were plotted and compared. Another parameter used in the study was the effect of near-fault versus far-field ground motion on strains in column and beam reinforcement. Lastly, the curvatures in the columns and beams were compared. Because the earthquake records have different characteristics, a comparable measure of the input and/or response was needed. The strain and curvature data were compared based on three measures: peak achieved shake table acceleration, spectral accelerations and drift ratios. In addition, drift ratio was compared for the peak achieved shake table acceleration and spectral acceleration measures.

2 TEST SPECIMEN AND SETUP

2.1 SPECIMEN DETAILS

The specimen represented a quarter-scale model of a prototype bridge bent in Las Vegas, Nevada. The scale was chosen so that the maximum specimen ductility could be achieved without exceeding shake table capacity. The specimen was of a unique design in that the columns had a diamond shape. The overall dimensions of the bent as well as cross-sectional views of the beam and column reinforcement are shown in Fig. 2.1.

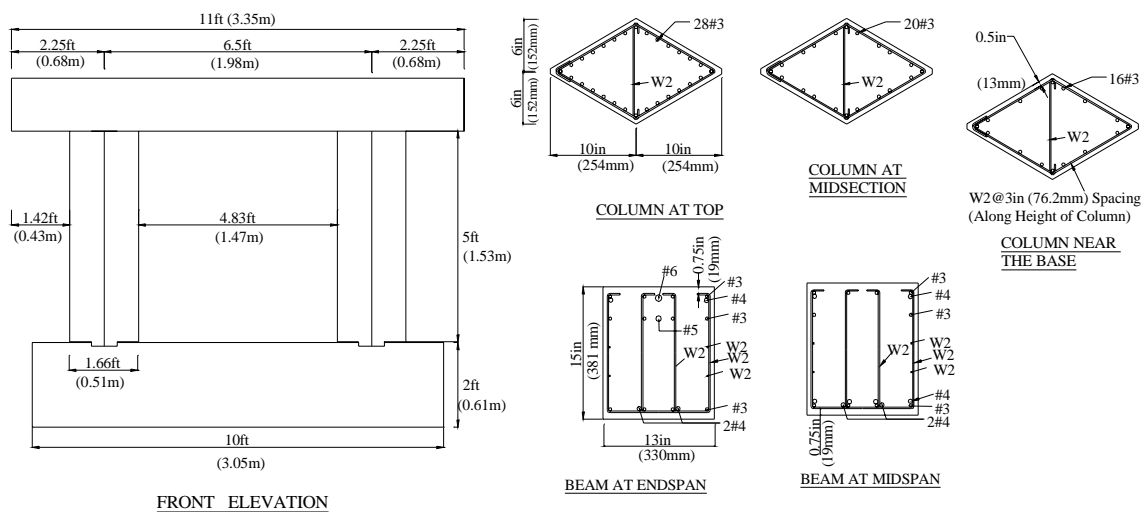


FIGURE 2.1 DETAILS AND DIMENSIONS OF THE TEST SPECIMEN

The footing was designed with the goal of having no yielding of steel and no cracking of concrete. This was done so that all of the deformation would take place in the columns and beam. The columns were detailed to act as two-way hinges at the base, which was the same as the prototype detail. The column longitudinal reinforcing steel consisted of #3 bars. The column transverse reinforcing steel consisted of W2 wires with a diameter of 0.161in (4.09mm). The ties were spaced at a distance of 3in (76 mm) along the height of the column, which made the confinement steel ratio 0.1%. The beam longitudinal reinforcing steel consisted of #3, #4, #5 and #6 bars, each with a yield stress ranging from 38.6 ksi (267 MPa) to 42.85 ksi (296 MPa). The beam transverse reinforcing steel consisted of W2 wire with the same properties as those of the column transverse reinforcement.

The two models, B2DA and B2DN had been constructed at the same time in 1/2003. B2DA was tested in 3/2003, but B2DN was saved for a future study. The average measured concrete compressive strengths of B2DA on the test day (when the model was 75 days old) are as follows; 6.25 ksi (43.1 MPa) for the footing, 8.08 ksi (55.7 MPa) for the column and 6.26 ksi (43.1 MPa) for the beam.

The columns and beam had several characteristics that classified them as substandard design. There was insufficient shear reinforcement in the columns and beams and the beam lateral bars were detailed as open stirrups. In addition, the beam-column joints had no shear reinforcement. Lastly, the amount of the confinement reinforcement was severely insufficient and the spacing was too large.

2.2 TEST SETUP

Testing was conducted at the Large Scale Structures Laboratory (LSSL) at the University of Nevada, Reno. The specimen was placed on the shake table and then grouted and tensioned to the shake table. Inertial mass was supplied through a translating frame named the mass rig. The mass rig was connected to the bent through a steel link. The vertical load was applied by ten hydraulic rams, each of which applied a force of 6.5 kips (28.9 kN) for a total axial load of 65 kips (289 kN). The vertical load was transmitted to the bent through a load transfer beam and ten threaded rods. For safety purposes, supports were placed on the sides of the specimen to prevent the specimen from collapsing in the out of plane direction during testing. The specimen was tested in the strong direction of the bent, which was the north-south direction.

3 TESTING PROTOCOL

Testing protocols for B2DN and B2DA were developed based on preliminary analytical studies. The purpose of the analytical studies was to select the input motion to be used for shake table testing. B2DA was subjected to the acceleration history recorded at the Sylmar receiving station during the 1994 Northridge earthquake. The Sylmar acceleration record has a peak velocity of 30.8in/sec (78.2cm/sec) and a peak acceleration

of 0.61g, and does not include the high velocity pulse due to the forward directivity effect. The distance to the epicenter was 8.45 miles (13.6 km). B2DN was subjected to the acceleration history recorded at the Rinaldi receiving station during the 1994 Northridge earthquake. The Rinaldi acceleration record is a near-fault ground motion with a peak velocity of 65.4 in/sec (166.1cm/sec) and a peak acceleration of 0.84g. The distance to the epicenter was 6.78 miles (10.91 km). The unscaled acceleration and velocity histories for these ground motions are shown in Fig. 3.1 and Fig. 3.2, respectively. The time scale for both ground motions was modified by a factor of 0.48 to account for the quarter-scale of the specimen and the slight difference between the vertical load on the bent and the inertial mass on the mass rig.

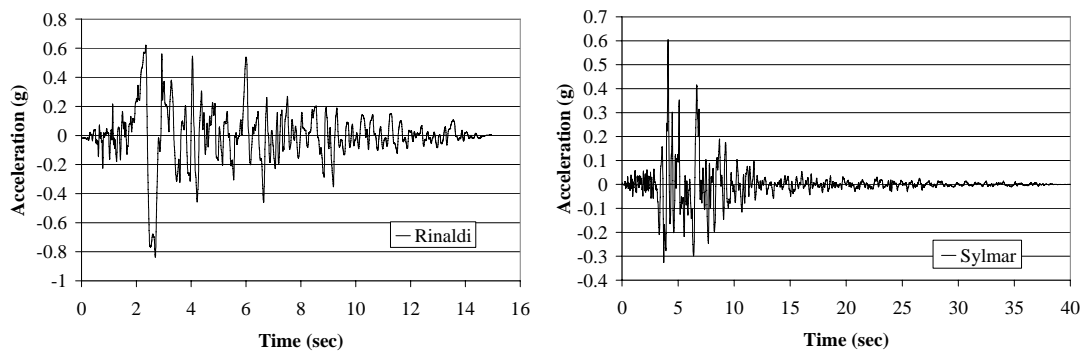


FIGURE 3.1 ACCELERATION HISTORIES

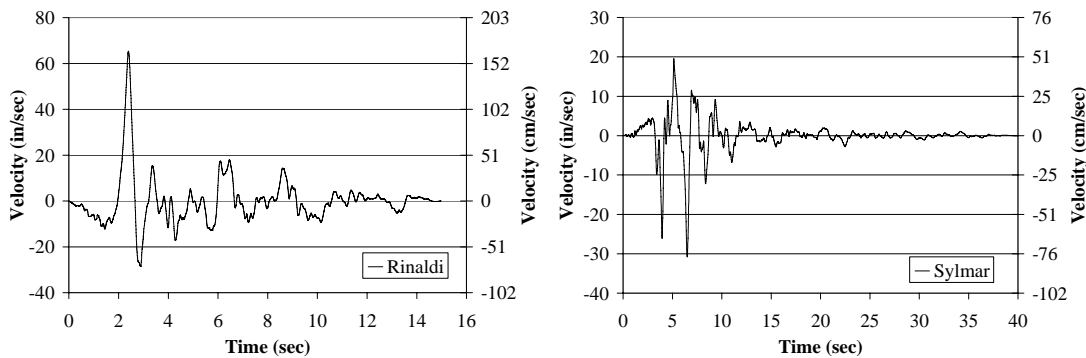


FIGURE 3.2 VELOCITY HISTORIES

B2DN was subjected to a total of four ground motions. The testing started out with smaller ground motions and increased in amplitude until failure of the specimen. It is essential to study the progressive deterioration of the specimen under increasing ground motion demand. However, the specimen was only able to undergo four ground motions because of the intense loading demand placed on the specimen by the near-fault ground motion. B2DA was tested in a similar fashion. However, it was able to undergo more ground motions because the far-field ground motion did not place as large of a demand on the specimen under smaller ground motions.

4 COMPARISON OF DAMAGE AND FORCE-DISPLACEMENT RESPONSE

4.1 VISUAL DAMAGE

Photos were taken of the specimens after each test run. The photos were used to document the visual damage to the specimens. Comparative photos of the south column from the final run of B2DN and B2DA are shown in Fig. 4.1-4.2, respectively. Both of the bents failed due to shear in the south column. From the photos it can be seen that the shear cracks in both models had the same angle but the one in B2DN opened wider than in B2DA and there was more concrete damage in B2DN at the upper left of the cracks. In addition, cracking is more extensive in the beam-column joint in B2DN than it is in B2DA. The cracking in the south end of the beam in both specimens appears to be similar.



FIGURE 4.1 B2DN 1.0xRINALDI



FIGURE 4.2 B2DA 2.25xSYLMAR

4.2 FORCE-DISPLACEMENT RESPONSE

A force-displacement curve gives insight to the overall performance of a structure. The measured force-displacement responses for B2DN and B2DA are shown in Fig. 4.3. It is evident from Fig. 4.3 that both models had a similar elastic stiffness. However, after the yield of the models, B2DN has a larger force response. It should be noted that both models maintained a similar displacement response. The above mentioned characteristics would tend to suggest that the near-fault ground motion had a greater impact with higher amplitude motions. This characteristic is also seen in the following sections of this paper.

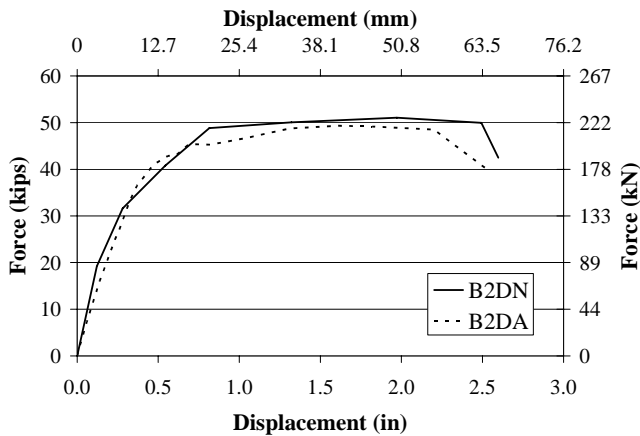


FIGURE 4.3 MEASURED FORCE-DISPLACEMENT RESPONSES

5 COMPARISON OF STRAINS AND CURVATURES

The objective of the test was to compare the effects of the ground motion type on the response of substandard two-column piers. In order to accomplish this, the maximum steel strains and member curvatures in B2DN and B2DA were compared. In this paper, only one critical longitudinal reinforcing bar is discussed. Transverse reinforcing bars were not examined because the strains in these bars were well below yield prior to the model failure and reached the rupture strain suddenly when the models failed in shear. The cross section at which the bar was located (section 1-1) is marked in Fig. 5.1. Figure 5.1 also shows the individual reinforcing bar that was examined at the section. This bar was chosen because it was at a location where the maximum moments take place in the structure. The maximum curvatures were also compared at section 1-1.

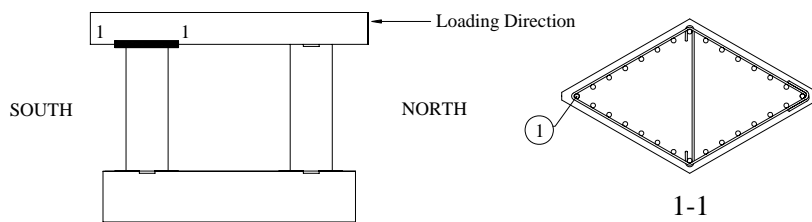


FIGURE 5.1 SECTION FOR STRAIN AND CURVATURE COMPARISON

Because the input earthquakes for the two test models had different characteristics, three different measures were used to examine the effect of input earthquake. These measures were peak achieved shake table acceleration, spectral acceleration at fundamental period of the test specimens, and the specimen drift ratio. These three measures were used because there are several different ways to compare ground motions and their effects. The peak ground acceleration (PGA) is generally used

as a measure of the intensity of the earthquake. However, PGA signifies intensity of earthquakes only when the ground motion characteristics such as duration and frequency contents are comparable. As a result comparison of the response based on PGA alone may be misleading. The spectral acceleration was also used as an index because this value represents the level of force that was applied on the specimen. The third measure was the lateral drift ratio, which represents the level of deformation of the structure. By considering these three measures it was hoped that a better insight on the effects of ground motion type would be obtained. Comparisons were made by calculating the percent change in strain and curvature between B2DN and B2DA.

5.1 PEAK ACHEIEVED SHAKE TABLE ACCELERATION

The peak achieved shake table acceleration was recorded for B2DN and B2DA during each run of testing. For each run of B2DN the peak achieved acceleration was determined and a comparable run with similar peak achieved acceleration was identified in B2DA. Table 5.1 lists the comparable runs.

TABLE 5.1 COMPARATIVE RUNS BASED ON PEAK ACHIEVED SHAKE TABLE ACCELERATION

B2DN Run Number	B2DN Achieved Motion x Rinaldi	B2DN Peak Achieved Acceleration (g)	B2DA Achieved Motion x Sylmar	B2DA Peak Achieved Acceleration (g)
1	0.37	0.31	0.51	0.31
2	0.60	0.50	0.84	0.51
3	0.80	0.67	1.07	0.65
4	0.94	0.79	1.18	0.72

It is apparent from Fig. 5.2 that near-fault ground motion increased the strain in the examined reinforcing bar. It is seen that the percent change in strain increased as the run number increased. This shows that under larger events the effect of near-fault ground motion on strain became more apparent. The average percent change in strain was 553%. Figure 5.3 shows that the columns curvature was also affected by the type of the earthquake, and that the near-fault motion caused considerably larger curvatures than those of the far-field motion. The average percent change in curvature was 133%. It is evident from the drift ratio comparison (Fig. 5.4) that the near-fault motion had a greater impact on B2DN than B2DA. B2DN consistently had a larger drift ratio than B2DA and with higher amplitude motions the impact became more significant. The average percent increase in drift ratio was 70%.

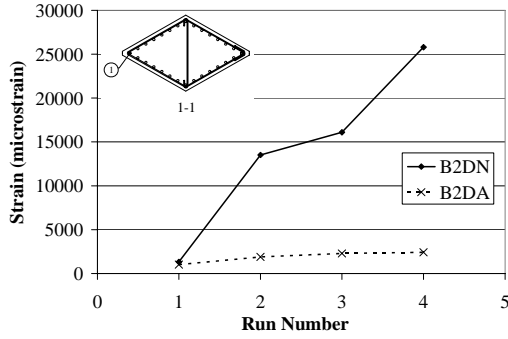


FIGURE 5.2 STRAIN COMP.

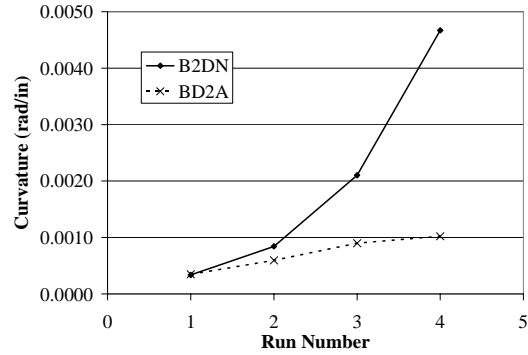


FIGURE 5.3 CURVATURE COMP.

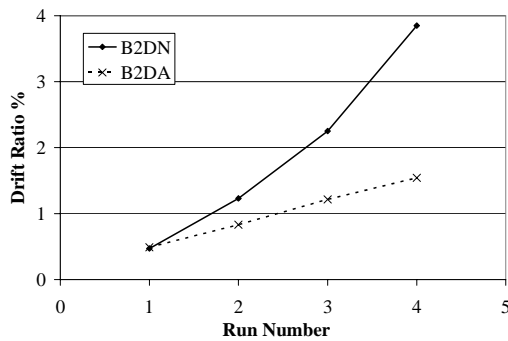


FIGURE 5.4 DRIFT RATIO COMP.

5.2 SPECTRAL ACCELERATION

Spectral acceleration is a measure of the force that is applied to the structure. For each run, the response spectrum was plotted and an acceleration value was determined based on the initial natural period of the bent (0.217 seconds). This period was determined from quick release tests on the day of shake table testing. For each run of B2DN the acceleration was determined and a similar acceleration was found from one of the runs for B2DA. Table 5.2 lists the runs that were compared based on runs one through four of B2DN. All of the runs for B2DN had a trend of increasing acceleration with run number except for run two, which consisted of the largest acceleration recorded. Thus, run two was omitted from the comparison because of inconsistency.

TABLE 5.2 COMPARATIVE RUNS BASED ON RESPONSE SPECTRA ACC.

B2DN Run Number	Input Motion x Rinaldi	Spectral Acceleration (g)	Input Motion x Sylmar	Spectral Acceleration (g)
1	0.25	0.92	0.24	0.88
3	0.75	0.97	0.48	1.00
4	1.00	1.41	0.60	1.30

Figure 5.5 shows consistent trends in the strain data and indicate substantial increase in strains under the near-fault earthquakes. The south column shows the trend of a larger percent change in curvature between runs as the input earthquake intensity increased. The average percent change in strain was 1198%, which is the largest for any of the intensity/response measures (the data for the drift ratio are discussed in the next section). The plot of curvature data in Fig. 5.6 shows trends that are generally similar to those of the strain data. The average percent change in curvature was 522%. It can be seen in Fig. 5.7 that B2DN experienced significantly higher drift ratios than B2DA. The average percent change in drift ratio was 330%, which is much larger than that for the peak achieved shake table acceleration comparison, but comparable to the strain and curvature data for this comparison.

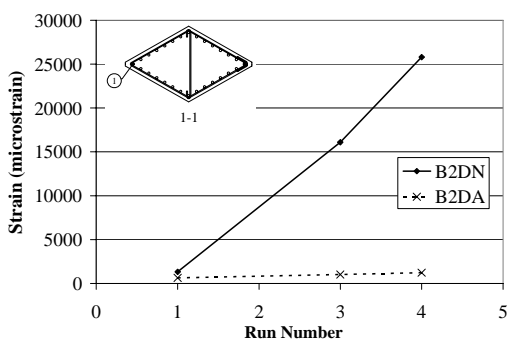


FIGURE 5.5 STRAIN COMP.

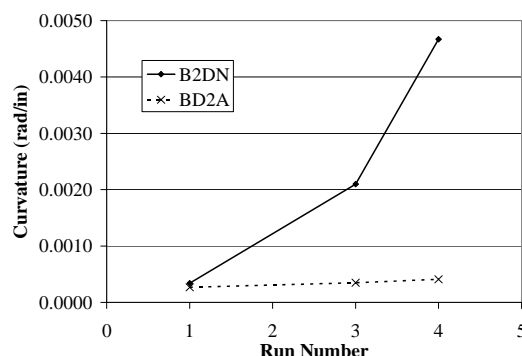


FIGURE 5.6 CURVATURE COMP.

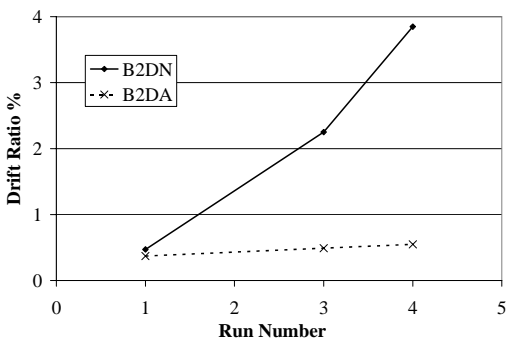


FIGURE 5.7 DRIFT RATIO COMP.

5.3 DRIFT RATIO

One measure of overall structural response is the lateral deformation. The bent lateral displacement relative to the shake table was measured for B2DN and B2DA during each run of testing. The drift ratio for the bent was calculated by dividing the bent displacement by the height from the top of the footing to the center of the beam. For each run of B2DN a drift ratio was determined and a similar drift ratio was found from a run of B2DA. Table 5.3 shows the runs with the same or nearly the same drift ratios for the two specimens.

TABLE 5.3 COMPARATIVE RUNS BASED ON SPECIMEN DRIFT RATIO

B2DN Run Number	Input Motion x Rinaldi	Drift Ratio %	Input Motion x Sylmar	Drift Ratio %
1	0.25	0.47	0.48	0.49
2	0.50	1.23	1.19	1.21
3	0.75	2.25	1.50	2.39
4	1.00	3.85	2.25	3.78

Figure 5.8 shows that the near fault motion increased the column bar strains. The average percent change in column bar strains was 153%. The column curvature data (Fig. 5.9), shows both specimens having a similar curvature for the first three runs and then B2DA having a larger curvature for the fourth run. The average percent change in curvature was -8%.

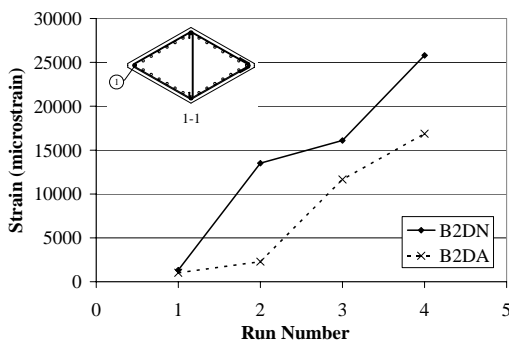


FIGURE 5.8 STRAIN COMP.

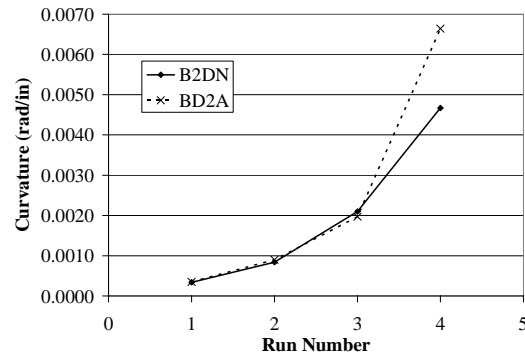


FIGURE 5.9 CURVATURE COMP.

6 CONCLUSIONS

The following observations and conclusions were drawn based on the data presented in this summary paper:

1. The near-fault, Rinaldi record caused more extensive apparent damage in the south beam-column joint and in the south column (the column that failed in shear in both specimens) than the Sylmar record in substandard piers.
2. The effect of near-fault ground motion tended to be more severe under higher-amplitude motions.
3. Regardless of the measure of input (PGA, spectral acceleration) or overall response (drift ratio) the near-fault motion led to generally larger strains, curvatures and drift ratios than those of the far-field motion on substandard piers. This suggests that the retrofit measures under near-fault motions might have to be more extensive than those under far field motions.

ACKNOWLEDGEMENTS

The study presented in this document was funded by the Federal Highway Administration (FHWA). The opinions expressed in this paper belong solely to the authors and do not necessarily represent the views of the sponsor. The valuable support of Dr. Patrick Laplace, Paul Lucas, Chad Lyttle, Hoon Choi, Arash Zaghi, Sarira Motaref, Ashkan Vosooghi and Kelly Doyle is much appreciated.

REFERENCES

1. Choi, H; Saiidi, S; Somerville, P; El-Azazy, S; "Bridge Seismic Analysis Procedure to Address Near-Fault Effects." Caltrans Bridge Research Conference, Sacramento, CA, Paper 02-501, October 2005.
2. Kawashima, K; MacRae, G; Hoshikuma, J; Nagaya, K; "Residual Displacement Response Spectrum." *Journal of Structural Engineering* 124.5 (May 1998): 523-530.
3. Park, S.; Ghasemi, H; Shen, J; Somerville, P.; Yen, W.; Yashinsky, M; "Simulation of the Seismic Performance of the Bolu Viaduct Subjected to Near-Fault Ground Motions." John Wiley & Sons, USA, 2004.
4. PEER Strong Motion Database. 2000. Regents of the University of California. <<http://peer.berkeley.edu/smcat/search.html>>
5. Phan, V; Saiidi, M; Anderson, J; Ghasemi, H; "Near Fault Ground Motion Effects on Reinforced Concrete Bridge Columns." Journal of Structural Engineering. ASCE, Vol. 133, No.7, July 2007, pp. 982-989.
6. Somerville, P.G. (2002). Characterizing Near Fault Ground Motion for the Design and Evaluation of Bridges. Third National Conference and Workshop on Bridges and Highways. Portland, Oregon. April 29 – May 1, 2002. <<http://www.peertestbeds.net/library/Ucs/GM/PaperonNearFaultGroundMotion.pdf>>.
7. Sureshkumar, K; Saiidi, S; Itani, A; Ladkany, S; "Seismic Retrofit of Two-Column Bents With Diamond Shape Columns." Civil Engineering Department, University of Nevada, Reno, Report No. CCEER-04-9, November 2004.